ZnO nanowires with Au contacts characterised in the as-grown real device configuration using a local multi-probe method

2014 Nanotechnology 25 425706

(http://iopscience.iop.org/0957-4484/25/42/425706)

OPEN ACCESS
IOP Publishing
Nanotechnology

Nanotechnology **25** (2014) 425706 (9pp)
doi:10.1088/0957-4484/25/42/425706

ZnO nanowires with Au contacts characterised in the as-grown real device configuration using a local multi-probe method

Alex M Lord[1], Alex S Walton[2,7], Thierry G Maffeis[3], Michael B Ward[4], Peter Davies[5] and Steve P Wilks[6]

[1] Centre for Nanohealth, College of Engineering, University of Swansea, Singleton Park, SA2 8PP, UK
[2] School of Physics and Astronomy, University of Leeds, Leeds, LS2 9JT, UK
[3] Multidisciplinary Nanotechnology Centre, College of Engineering, University of Swansea, Singleton Park, SA2 8PP, UK
[4] Institute for Materials Research, University of Leeds, Leeds, LS2 9JT, UK
[5] Scientific Imaging and Analysis Facility, College of Engineering, University of Swansea, Singleton Park, SA2 8PP, UK
[6] Multidisciplinary Nanotechnology Centre, Department of Physics, College of Science, University of Swansea, Singleton Park, SA2 8PP, UK

E-mail: a.m.lord@swansea.ac.uk

Received 11 July 2014
Accepted for publication 26 August 2014
Published 3 October 2014

Abstract

We demonstrate here a method using a multi-probe UHV instrument to isolate and measure individual metal contacts controllably fabricated on the tips of free standing ZnO nanowires (NWs). The measurements show Au can form reliable Ohmic and rectifying contacts by exercising control over the surface properties. In the as-grown state the Au contacts display low-resistance characteristics which are determined by the adsorbed species and defects on the NW surface. Subjecting the NWs to an oxidising agent (H_2O_2) increases the surface potential barrier creating more rectifying contacts. These developments are crucial for controllable NW array devices.

S Online supplementary data available from stacks.iop.org/NANO/25/425706/mmedia

Keywords: nanowires, electrical contacts, scanning tunnelling microscopy, Ohmic, rectifying, ZnO

(Some figures may appear in colour only in the online journal)

1. Introduction

The one dimensional morphology of nanowires (NWs) and the properties of ZnO provide significant advantages in applications such as room temperature UV lasing [1], gas or chemical sensing [2], and field effect transistors (FETs) [3]. High electromechanical piezoelectric coupling of ZnO NWs has also led to the development of highly sensitive transducers and actuators [4]. These nanosensors often exhibit superior performance to bulk-based sensors due to the

[7] Present address: Interdisciplinary Nanoscience Center (iNano), Aarhus University, Gustav, Wieds Vej 14, DK-8000 Aarhus C, Denmark.

dominance of the surface properties, and the ability to produce high quality single crystal structures at the nanoscale. However, the electrical properties of such nanostructures are very difficult to assess when the surface has such a major influence making measurements extremely sensitive both to pre-measurement processing steps and to the configuration in which the measurements are made. For instance, most techniques for measuring nanostructure properties require the fabrication of specific device structures (such as a FET), that often involve complex lithographic processing steps before any measurement can be made [5]. These processes result in the deposition of organic impurities on the surface that have a significant effect on the intrinsic properties of the nanostructures [6]. Furthermore, many of the ground-breaking devices [7, 8] are based on vertical arrays of NWs or nanotubes emerging from a substrate [9], hence their properties are not well represented by measurements of flat-lying single-structure devices with end patterned contacts. It is thus critical to characterize the materials in their as-grown vertical configuration. This realization has led to recent studies advancing the characterization of vertical as-grown NWs with methods that are free from sample processing, and in particular, investigating the behaviour of electrical contacts to the free tips of the vertical NW arrays [10–12]. A major limiting factor of these recent techniques is the current path always involves passage through a supporting substrate on which the NW arrays have been grown. Therefore, the intrinsic properties of the NW, or a contact formed to the free standing end of the NW, maybe masked by the influence or dominance of the NW–substrate junction that may introduce unquantifiable scattering events, current spreading, thermal losses and crowding of the potential energy field. Here we use a multiple probe method that overcomes this problem and achieves a configuration in which the intrinsic properties of the NW and a contact formed to the NW tip, can be studied in the as grown array.

How can free-standing nanostructures be measured in isolation without modification or damaging processing steps?

The major challenge to overcome is the ability to approach and form multiple contacts simultaneously to a single free standing vertical NW in such dense arrays. Recent methods have had some success by employing a single probe to contact the metal alloy tip that resides on the top of the NW after metal catalysed vapour phase growth [11]. Léonard *et al* performed electrical measurements on Ge NWs using a Au coated tungsten probe installed in a scanning electron microscope (SEM) and found the catalyst contacts became more conductive as the NW diameter was reduced below 60 nm. With a similar single probe experimental configuration, Timm *et al* have performed experiments with a scanning tunnelling microscope (STM) to show Au catalyst particles provide Ohmic contacts on In–P and In–As NWs [10]. However, all of these studies required the current to flow not only through the metal–NW interface, but also through the NW–substrate junction where modifications to the sample structure were necessary to make the latter interface Ohmic; the substrate material was made identical to that of the NW, but with n^+ doping. Such constraints are not always compatible with real device structures and can also induce diffusion of dopants into the NW, perturbing the intrinsic or intended properties. A more satisfactory experimental setup is with one probe contacting the metal at the free end of the NW and a second probe in direct Ohmic contact with the NW further down its shaft allowing the NW and its interface properties to be studied in its natural device-like configuration. Herein we demonstrate a technique for ZnO NWs and their electrical contacts which addresses the shortcomings of the existing approaches, namely: (1) fabrication techniques that unintentionally change the surface properties, (2) alteration of the growth structures to be conducive to the measurement technique, (3) measurement across a structure containing more than one material interface and of various dimensions, and (4) difficulty in knowing the precise point of contact between probe and NW. We overcome these major challenges by applying a UHV multi-probe system with *in situ* SEM to free standing NWs of diameter 50 nm–300 nm. Multi-probe instruments with probes of various materials and configurations have been successfully used to characterize the electronic properties of one- and two-dimensional materials such as GaN NWs [13] and carbon nanotubes [14, 15] particularly by Li and co-workers at Oak Ridge National Laboratory. However, it is possible to use such a technique to measure as-grown NWs and assess the electrical contribution each wire makes to a device in the array configuration [16]. Here, we provide a detailed description of the multi-probe measurement technique to measure NW top contacts and study the properties of Au deposited on the tips of single vertically-standing ZnO NWs in the original growth array. The measurements reveal the Ohmic nature of the junction which has predictable behaviour; however, rectifying contacts are also crucial when designing a device. With this objective in mind, we investigated the formation of rectifying contacts using the same Au contact metal by applying a chemical treatment to the ZnO NW surface which modifies the interface properties.

2. Experimental methods

2.1. NW growth

Single crystal sapphire substrates for defect-driven growth were cleaned with solvents and rinsed before etching in NaOH (1 M) for 5 min [16]. After etching, the substrates were rinsed thoroughly with DI water, ethanol and a further water rinse and dry. Etching was performed with stirring at room temperature. NW growth was performed in a tube furnace with the following experimental parameters—furnace temperature 1050 °C, substrate temperature 600–650 °C, pressure 1.6 mbar, gas flow 100 sccm Ar and 10 sccm O_2, growth time 60 min. To achieve a high purity Zn vapour the source materials were ZnO (Alfa Aesar 99.99%) and carbon (sigma Aldrich 99.99%) 325 mesh.

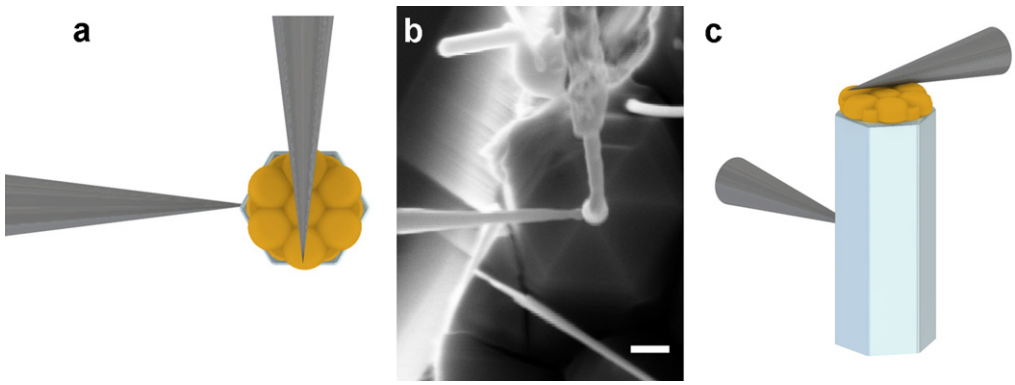

Figure 1. Schematic diagrams and a SEM image to describe the configuration in which a measurement was performed. (a) shows the top–down perspective seen in the SEM image shown in (b), an *in situ* SEM image (scale 200 nm) and visualized using (c) a scale 3D representation of the measurement setup with two tungsten probes in contact with a ZnO NW.

2.2. Contact fabrication

Au was evaporated onto vertical catalyst-free NWs using an Edwards thermal evaporator at 10^{-5} mbar and observed in transmission electron microscopy (TEM) to characterize the Au thickness and crystallinity. The NW array was secured at a known height above the source basket with the NWs perpendicular to the sample plate.

2.3. NW and contact characterization

SEM was used to examine the products from each growth experiment, particularly the morphology, alignment and areal density. The SEM used in this study was the Hitachi S4800 cold field emission gun SEM equipped with YAG BSE backscatter detector of resolution 3 nm.

The TEM used in this work was a FEI Tecnai TF20 FEGTEM which operates at 200 keV with a selected area aperture for diffraction patterns. NWs were transferred from the growth array directly to a holey carbon coated Cu grid (400 mesh Agar Scientific) without the use of an intermediate solvent.

2.4. Electrical measurement

The Omicron UHV Nanoprobe comprises four individual W probes guided by a high resolution Gemini FEG–SEM. By guiding the four STM probes with the SEM it is possible to form reversible, non-destructive electrical contacts to an individual nanostructure. The electrical measurements were conducted with a Keithley 2601 source meter with a measurement range of picoamp to Amp. The probes were electrochemically etched in KOH (2 M) with 15 V dc supply applied through the 0.25 mm W wire. The NW arrays were loaded into the load lock of the nanoprobe and pumped down until the vacuum pressure of 10^{-9} mbar was reached. Experiments were conducted at pressure 10^{-10} mbar. Using the *in situ* SEM imaging and full STM piezo control the probes were positioned close to the surface after the probes had been current annealed to remove oxides and contaminants. The *in situ* SEM (resolution <5 nm) images were used to measure the NW diameter with an error of ±2.5 nm.

3. Measurement and characterization of NW contacts

3.1. Measurement of NWs

The power of the measurement technique was in the ability to measure nanostructures in their as-grown state once they had been loaded into the UHV instrument as shown in figure 1. In the main UHV chamber with the sample on the measurement stage, initial observations using the *in situ* SEM enabled a suitable free standing NW to be identified and allowed the diameter to be accurately measured (resolution <5 nm). The SEM viewpoint provided a top–down perspective of the vertically grown NW array (as shown in supplementary figure S1) allowing placement of the tungsten probes under piezo-motor control, enabling a soft landing and avoiding damage to the probes or the NW of interest. This was achieved with a manual stepwise and iterative approach to lower the probes near to the sample as it was not possible to use the STM current feedback function with such a highly irregular surface. During this initial lowering procedure, the probe to sample surface separation was estimated by identifying the change in focal point of the SEM image between the NW tip and the measurement probes that pointed downwards at 45°. The initial objective to ensure accurate electrical measurement of the undisturbed contact was to lower the two probes close to the NW height and firstly contact either side of the NW with both of the probes. To achieve this configuration, on initial placement the first probe had been brought close to the height of the NW tip with the coarse motors and then the fine-piezo controls were used to lower the probe nanometre by nanometre in the *z*-direction adjacent to the NW side. The correct height was confirmed when the probe was observed in the SEM image to gently deflect the NW when the probe was moved with the *x*- and *y*- fine-piezo controls, and then the second probe was lowered in a similar manner. This process avoided the need to use the Au contact as the initial landing point which could disrupt the metal and positioned the probes approximately 1 μm from the NW tip whilst also ensuring no additional current path was formed by touching another NW. Once the probes were in satisfactory contact with the NW side facets, the SEM beam was turned off, the sample set at

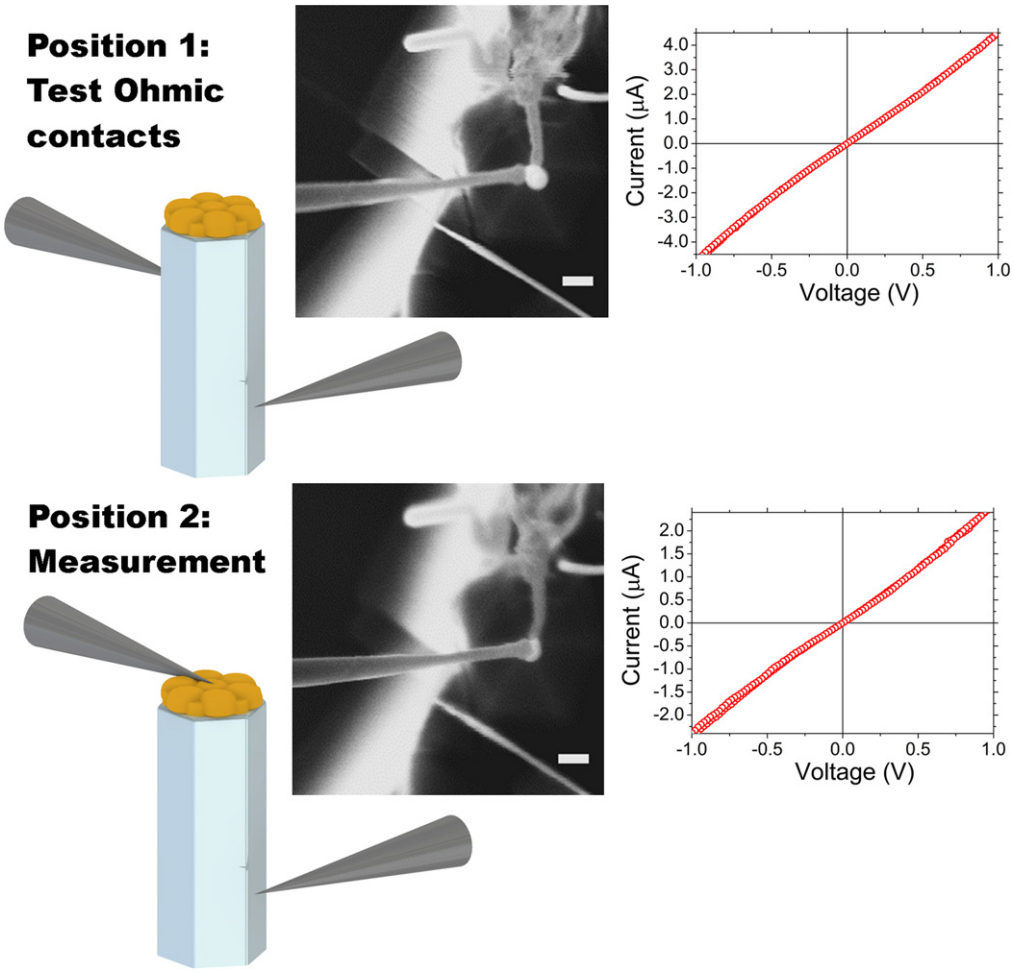

Figure 2. The figure presents a graphical description of the necessary stages in taking a measurement. Position 1 shows two probes both in contact with the sides of the NW (diameter 100 nm), as shown by the scale drawing and the top–down SEM image (scale 200 nm). In position 1 it is possible to test the probe contacts to make sure they are conductive and without an appreciable potential barrier, i.e. the contacts are Ohmic as shown in the corresponding *I–V* graph. Establishing the Ohmic contacts on the NW side enables one probe to be lifted and placed onto the NW tip as shown in position 2 by the scale drawing and *in situ* SEM image. When the probes are in position 2, a measurement of the top metal contact is then performed safe in the knowledge the side probe contact will not have a substantial influence on the *I–V* characteristics. For the case of Au deposited onto ZnO NWs an Ohmic contact is formed, as shown in the corresponding *I–V* graph.

floating potential and an *I–V* measurement was taken by grounding one probe and sweeping the voltage (±1 V) of the other. This provided a test of the probe contacts on the NW which were usually highly conductive (microamp current) and with linear *I–V* characteristics (this initial probe configuration and the corresponding *I–V* data are shown in figure 2 as position (1). Testing the contacts in this way ensured Ohmic contacts had been formed on the NW side that were necessary to accurately determine the properties of the top contact. This ability to form an Ohmic contact in such close proximity to the top contact and directly on the structure of interest removes all perturbations that may result from the NW substrate. Furthermore, although the probes were etched in a similar way to STM probes they were not atomically sharp, having a probe diameter comparable to that of the NW. This increased the contact area making the probe contact properties more stable. A greater voltage range was not used as the high current (>10 μA) can lead to electrical breakdown in ZnO NWs.

On formation of the side Ohmic contacts the SEM beam was turned on, the sample was grounded and the second probe (that was within fine-piezo range (<1 μm) of the NW tip) could be removed from the NW and maneuvered above the Au contact as shown in figure 1. Once the probe was above the NW a small bias was applied to the probe (0.1 V) and lowered in nanometre steps until a spike above the noise (pA) was observed in the current, this is the equivalent of an automated tunnelling feedback approach. Approaching a NW contact in this way with a bias applied to the probe can lead to axial stretching, but this was avoided by using a bias significantly below the limit that will cause appreciable deformation and can be considered as a soft touchdown onto the NW with no observed deflection [17]. As an additional measure the probe was kept at a constant height once the circuit was complete. Interestingly, with careful manipulation it was possible to deflect the NWs and bend them double without failure, showing the tremendous mechanical properties of single crystal NWs. However, to avoid the confusing

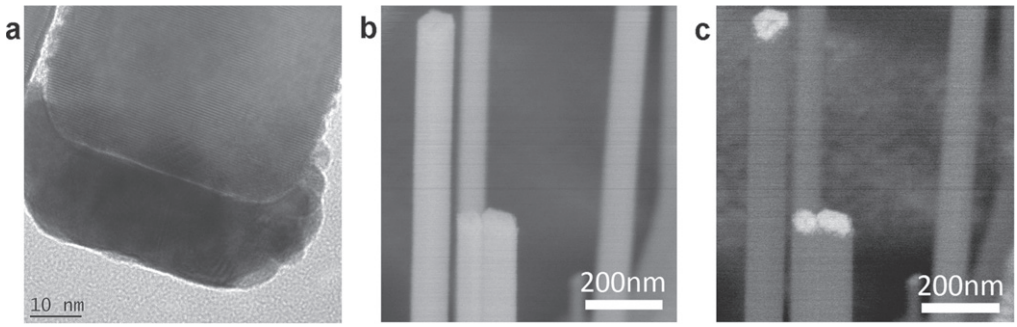

Figure 3. Electron Microscopy images of the ZnO NWs with Au top contacts. (a) TEM lattice image of a ZnO NW with a 20 nm thick Au pad on the end (0001) facet. (b) SEM image of vertical NWs with 10 nm thick Au contact pads on the top facet and in (c) the same NWs shown with BSE imaging which highlights the Au pad on the top facet and the side facets are clean.

effect of piezoelectric potential in ZnO, measurements were conducted with the NW observed to be in the original vertical position. *I–V* measurements were then performed with the Ohmic probe contact on the NW side and the other probe on the Au contact (shown in figure 2 as position 2); it was not necessary to bed the probe further into the metal to establish an appreciable current (μA) across the contact. To ensure the measurements could be repeated the probe was lifted from the Au contact and then lowered again with real-time current monitoring and the *I–V* measurement was repeated several times. The final measurement configuration is shown in figures 1(a)–(c). A distinct advantage of the combined SEM–STM approach is the ability to know the exact position of the probe and whether it is in contact with the metal overcoming the large uncertainties associated with single probe techniques. However, as with all electron microscopy techniques, care needs to be taken to prevent beam deposited carbon contamination, which we avoided here by removing any sources of hydrocarbons from the measurement chamber. When contamination was a problem a significant drop in current magnitude was observed and only current in the <10 nA range was measured at an applied bias of ±1 V, also previously observed during four probe measurements of similar NWs [12]. When contacting such small structures there are also physical limitations placed on the measurement procedure that are predominantly concerned with the NW growth density. It was found for most growth arrays that NWs could be approached within the centre of the array as the probe angle of 45° enables a reasonable probe extension (∼1 μm) along the structure length for NW spacing <1 μm. For the densest arrays, measurements were conducted along the edge of the NW array which allowed an easy approach of the probes onto close-packed NWs and subsequently multiple probe positions were possible on a single NW (an example is shown in supplementary figure S2). The most problematic NWs to measure were those of high aspect ratio >50 due to their flexibility, however, NWs of diameter 50 nm were successfully measured in this study. Therefore, utilizing this accurate method, the measurements were repeated on several NWs across a range of diameters and growth arrays.

3.2. Contact characterization

Non-catalysed ZnO NWs are known to be of high quality with predictable composition, structure, and morphology. The vapour growth method used here occurred without a specific catalyst and at temperatures much lower than metal catalysed growth, typically the substrate was located in the temperature range ∼600 °C [8, 18–20] and growth was induced by a process of crystal nucleation on the intended substrate via a vapour–solid mechanism [16]. Initial growth can be encouraged by providing preferential nucleation points on the substrate either by creating surface roughness or with a crystal seed layer [20]. Combining this technique with lattice matched substrates, such as the a-plane sapphire used here, results in high quality vertically aligned NWs that are ideal for devices and fabricating controlled top contacts. Two techniques for fabricating the contacts were tested for the quality of the deposition which was assessed with electron microscopy to examine the metal pads that were formed. Firstly, plasma assisted magnetron sputtering was found to coat not only the NW tips but also the NW side facets creating a short circuit path along the NW surface. To overcome this problem thermal evaporation was chosen as it is known to provide unidirectional deposition especially at the large working distances (∼30 cm) that are possible with bell jar evaporators [22]. The metal deposition was achieved without resorting to resist processing techniques that can otherwise be useful for protecting or embedding the NWs [23], but in this instance it was crucial to avoid these processes to prevent surface modification and hence, reveal the intrinsic properties of the NW-contact system. Noble metals make useful contact materials, Au was chosen here, as they are not subject to oxidation when exposed to air and on planar devices Au is known to form a large Schottky barrier with ZnO (0.6 eV) [24]. It should be noted that after growth it was necessary to expose the NWs to atmosphere before and after loading into the evaporation chamber thus exposing the ZnO surface to water vapour, oxygen and other environmental species. In the instance of ZnO NWs measured here no treatment was performed before Au pads of various thicknesses were deposited directly onto the untreated arrays to test any relationship with contact thickness; a 20 nm thick pad is shown in figure 3(a).

Examining the product of the fabrication process with TEM showed a pad of dense Au particles forming a suitable contact that always covered the entire width of the end facet of the single crystal NW. During characterization, the NWs were observed to always maintain parallel sides and along with the excellent alignment of the NW growth array these were crucial characteristics to obtain a flat Au pad on the NW tip and minimal coverage on the NW side facets. The tightly packed Au nanoparticles did not have any crystallographic alignment with the NW and appeared to have random orientation; however, the shape of the Au contact pads was uniform and conducive to physical contact and probe measurements, forming a robust layer. To ensure a short circuit path did not exist along the NW wall, a Hitachi S4800 SEM with YAG BSE backscattered electron (BSE) imaging was used to investigate the deposition of Au on the vertically standing NWs that were eventually used for the electrical measurements (figure 3). The BSE image in figure 3(c), where the intensity of the signal is largely dependent on the material composition, shows a distinct Au contact on the NW tip and no Au further along the NW shaft. This is difficult to assess with secondary electrons alone, figure 3(b).

4. Results and discussion

Once the structural quality of the contacts had been confirmed it was possible to conduct the electrical measurements with the optimum procedure of manipulating the probes with manual piezo-motor control. The electrical measurements spanned across several samples of NWs with diameters up to 300 nm and Au depositions of ~10–20 nm thickness, initially a total 20 NWs from five different arrays (same experimental parameters) were measured. Figure 4(a) shows three typical *I–V* measurements of NWs deposited with 10 nm, 15 nm and 20 nm Au on NWs of diameter 42 nm, 63 nm and 110 nm respectively with the three examples showing little deviation from linear *I–V* characteristics that are the hallmark of Ohmic conduction. Similar *I–V* characteristics were seen with all of the Au–ZnO NW contacts measured; no *I–V* measurement indicated a substantial potential barrier at any Au thickness or NW diameter. Ohmic contacts are crucial in all electronic devices as they do not present a potential barrier to the flow of current making them appropriate for charge injection, although they still have a contact resistance associated with the metal (probe/Au) and semiconductor (NW) interface. As for any low-resistance contacts, it is necessary to quantify the contact resistance of the Au contacts. The two-probe method in position 2 provides a measure of the resistance between the two W probes where the total resistance $R_{\mathrm{Total}} = R_{\mathrm{W}} + R_{\mathrm{NW}} + R_{\mathrm{Au}}$ with R_{W} the probe–NW contact resistance, R_{NW} the intrinsic NW resistance and R_{Au} the metal contact resistance. It is not possible to extract these three values from the two probe measurements alone. Therefore, using our previous four probe measurements on ZnO NWs [12], that showed the W probes form Ohmic contacts on the wires, it is possible to extract the W probe contact resistance R_{W} from each four probe measurement along with the intrinsic NW resistance R_{NW} using a channel length of 1 μm. This provides an expected range of values for R_{NW} and R_{W}, as shown in supplementary figure S3, for NW diameter range (<120 nm). In this size range, of the 15 Au tipped NWs that were measured here, 12 NWs had R_{Total} within the expected range of R_{NW}, showing for these measurements R_{W} and R_{Au} are similar in magnitude or less than the intrinsic properties of the NWs. However, three NWs exhibited a resistance R_{Total} considerably greater than the measured four probe range of R_{NW} or R_{W}. Therefore, the difference between the expected range of R_{NW} and the measured R_{Total} can be used to estimate R_{Au} for those three NWs, and determine a specific contact resistance range of between $5 \times 10^{-5}\,\Omega\,\mathrm{cm}^{-2}$ and $4 \times 10^{-4}\,\Omega\,\mathrm{cm}^{-2}$, which compares favourably to many Ohmic contacts to ZnO (this is described in more detail in supplementary figure S3 with an accompanying description) [24].

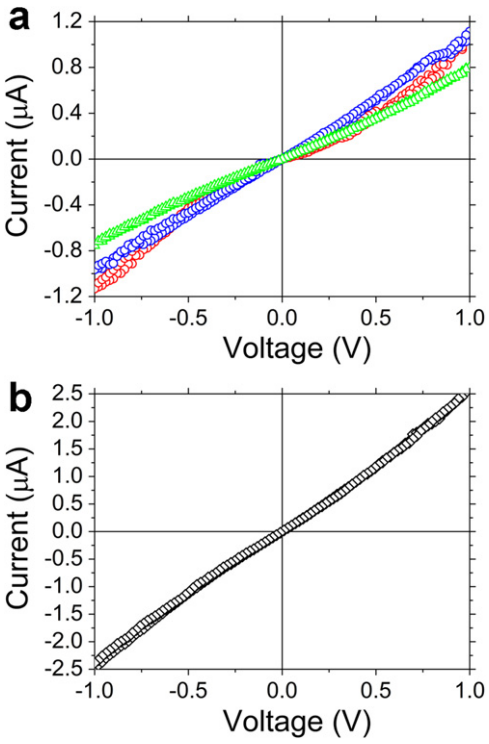

Figure 4. The *I–V* measurements of free standing as-grown NWs. (a) NWs with Au deposition thickness of 10 nm (green), 15 nm (blue) and 20 nm (red), on NWs of diameter 42 nm, 63 nm, and 110 nm respectively. (b) A 95 nm diameter NW with no Au deposition. All NWs measured showed similar linear *I–V* characteristics.

The observed variations in current magnitude (figure 4) in this case can be attributed to differences in resistivity from NW to NW. More crucially, the stand out feature of the *I–V* measurements is the linear behaviour which appears unusual for Au contacts on ZnO when the contact material is more commonly associated with rectifying junctions. Indeed, for UHV formed contacts on the cleaned pristine ZnO surface a large Schottky barrier is always measured with Au, so what is the effect that completely overrides this property? To answer this we must consider the reactive nature of the ZnO surface and the effect of trap states on the electronic properties. It is known that under NW diameters of 120 nm variations in

surface state density induce a large spread in conductive properties for similar ZnO NWs, changing the resistivity by two orders of magnitude 0.02–2 Ω cm [12, 25]. The surface effect originates from exposure of the ZnO to air resulting in a reaction with atmospheric gases such as oxygen trapping charge carriers at the surface creating a surface depletion region and a reduced conductive core; this was previously confirmed by four-probe measurements of NWs [12] in similar UHV conditions to those used here. The adsorbate layer creates a potential barrier, for which a typical measured value is ∼0.2 eV when the NWs are exposed to air [25], providing a useful guide for the NWs measured here. To emphasize the influence of the surface, the Au deposition occurred at $\sim 10^{-5}$ mbar and as such the removal of adsorbates will not be as comprehensive as compared to UHV, with any adsorbate layer being trapped at the Au–NW contact interface. It should be noted in all investigations the ZnO NWs have never been observed to have an amorphous surface layer and consistently the unbroken Zn lattice planes extend to the NW surface when inspected with TEM. The electron microscopy analysis has shown the NWs are defect free, growing along [0001] with a hexagonal cross-section. This observation coupled with the high quality of the ZnO NWs that have been shown, within the limits of TEM analysis, to have clean and abrupt (0001) top facets leaves the adsorbate buffer as the only remaining influence between the Au and ZnO. However, when the formation of Schottky diodes is considered in more detail it is widely apparent that the interface structure can have an overriding effect on the electronic characteristics.

High quality Schottky barrier fabrication usually takes place in UHV conditions when the surface has been prepared by cycles of annealing and ion-bombardment to remove oxides, water and tightly bound gases. Additional to this surface conditioning, oxygen plasma treatment of bulk and planar ZnO is common practice which removes surface and sub-surface defects, surface adsorbates and hydrogen that can act as a surface donor through hydroxyl formation [21, 26]. The reduction in native point defects at or near the ZnO surface that results from the oxygen plasma treatment has been shown by Brillson *et al* to be the more crucial effect in producing rectifying Au contacts. Structural inhomogeneity on an atomic scale is known to exist on the (0001) facet of ZnO which is more catalytically active than the oxygen terminated and negatively charged $(000\bar{1})$. This feature induces the growth of NWs in a reaction process which is encouraged by the activity of the positive Zn^{2+} (0001) top facet in a vertical NW array [27, 28]. Diebold *et al* have shown the polarity of the ionically bonded wurtzite ZnO requires a stabilizing reduction in charge of the positive Zn terminated (0001) top facet by ∼1/4 with negatively charged oxygen atomic steps and islands [29]. These atomic anomalies on the terminating facet may induce local variations in intrinsic surface states and trap density while influencing their energetic location (possibly within the bandgap), resulting in lateral barrier inhomogeneity and increased tunnelling [30, 31]. Overall, the combination of surface defects, native defects and surface adsorbates leads to band bending and a barrier height that is not solely the result of contact with the metal. Consequently, the current did not exhibit diodic behaviour. At this point it is worth considering the present knowledge of nanoscale ZnO which shows that a surface reaction occurs resulting in a surface depletion region, this appears contradictory to studies of bulk ZnO in vacuum where surface accumulation on the polar (0001) and $(000\bar{1})$ has been revealed due the presence of hydrogen [32]. However, this comparison appears to be a simplistic view because the as-grown NW carrier concentration (10^{17}–10^{18} cm^{-3}) is known to exceed that of the bulk crystal (10^{15} cm^{-3}–10^{17} cm^{-3}), indicating that some fundamental difference exists. Additionally, the non-polar NW side facets that create the diameter dependent electronic properties are only tens of nanometres in width, potentially exhibiting a different surface structure to large bulk or planar crystals. Revealing the mechanisms behind this behaviour will allow the models of bulk and nanoscale ZnO to agree and will greatly enhance the control over contact behaviour and conduction properties. To rule out other possible influences on the observed *I*–*V* characteristics we include measurements on bare NWs (figure 4(b)) which all showed the same Ohmic nature as the NWs with fabricated contacts confirming the semiconductor is decoupled from the deposited metal. To show the conduction mechanisms were not only short path effects, supplementary figure S4 shows the *I*–*V* characteristics when the probe is placed on the NW tip and the current path (several mm) was completed by the large area contact to the side of the NW array. This indicates we have identified and fabricated reliable and reproducible Ohmic contacts to individual free-standing ZnO NWs which is a crucial step towards high quality devices. These findings also confirmed for the general case of Au Ohmic contacts on ZnO the decoupling of the surface barrier from the metal can be caused by exposure to air [26]. The buffering effect offers an easy method for fabricating repeatable and reliable Ohmic contacts to all ZnO NWs; however, it makes the process of creating and controlling Schottky diodes a more complicated proposition.

For other NW materials such as Ga–As progress has been made in reducing the barrier height to 0.35 eV of pinned Schottky contacts by controlling the electrostatics of the interface with the materials composition [33]. Applying a wet chemical approach here achieved an increase in the rectifying nature of the Au contacts by exposing the ZnO NWs to 5% H_2O_2 for 10 s, a technique which has been successfully applied on planar ZnO [34] (A concentrated treatment was not chosen to avoid etching of the NWs and reducing the structural quality or creating an additional surface compound). Effectively, we have begun to exercise control over the contact properties without changing the contact metal or NW composition. Exposing the NWs to H_2O_2 has a similar effect to oxygen plasma by reducing native point defects, reacting with adsorbates that can act as donors and increasing oxygen radicals near the surface [5, 34, 35]. This has two effects on the NW: (1) an increased concentration of carrier traps and/or reduction in Oxygen vacancies on the surface creates a larger surface potential barrier; (2) the reduction of carriers increases the NW resistivity, this is more pronounced for NWs below 120 nm in diameter [12]. Importantly, the resulting effect was

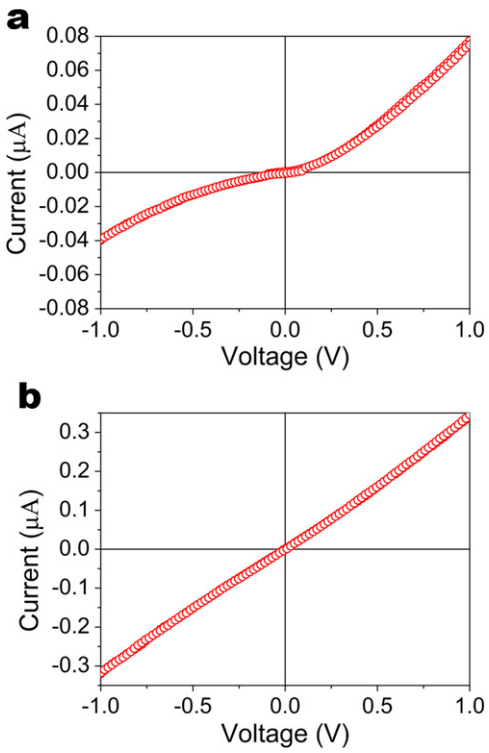

Figure 5. The *I*–*V* measurements of a free standing as-grown NW (diameter 110 nm) treated with H_2O_2 before Au contacts were deposited at a thickness of ~12 nm. (a) Shows the increased rectification of the Au contact with the probes in measurement position 2. (b) Shows the initial Ohmic contacts formed on the side of the NW in probe position 1.

to change the nature of the Au contacts so they became more rectifying (figure 5(a)) [26, 34]. The contacts are not yet ideal Schottky contacts, this is most likely due to the nanometre scale of the contacts and the limited concentration of the H_2O_2 treatment that is possible without depleting the entire NW. Importantly, the modification of the contact behaviour is notable progress for a highly sensitive material like ZnO which is susceptible to harsh processing [34]. Additionally, achieving an increase in the rectification ratio presents the concept that control over NW contact function can be obtained by surface chemistry alone. Crucially, the surface treatment that created a more substantial potential barrier did not inhibit the ability to form Ohmic contacts on the sides of the NWs (figure 5(b)); albeit, with lower measured current than those that were typically recorded for the untreated NWs (μA). Examining structures over a range of sizes (further measurements are discussed in supplementary figure S5) shows that thinner NWs (<120 nm diameter) exhibited higher rectification and lower current density as the effective carrier concentration was reduced to a greater extent than the thicker NWs (this is displayed by the current density plot in supplementary figure S6). The overall effect of the treatment on the wires created a greater potential barrier at the Au contact providing bias dependent carrier transport across the junction.

5. Conclusions

We have shown with a multi-probe technique that the action of surface states on ZnO NWs make it possible to form predictable, high quality Ohmic contacts with inert metals. Additionally, when exercising control over the surface the nature of the contact can be defined, rectifying or Ohmic even with the same contact metal. Further work will explore surface modifications that will improve the rectification of the contacts. The measurement technique overcomes the shortcomings of existing single probe methods to allow direct measurement of the structure or interface of interest by forming non-destructive reversible contacts locally on the structure. This is an important and necessary tool to enable the optimization of enhanced nanodevices, especially those utilizing arrays of NWs.

Acknowledgements

Leeds EPSRC Nanoscience and Nanotechnology Facility (LENNF) is an EPSRC funded user facility based at the University of Leeds, and provided TEM and Nanoprobe access. A. Lord would like to thank B. Palmer of the Weizmann Institute, IL, and Q. Ramasse of SuperSTEM, UK, for their invaluable contributions in formulating the discussions in the article.

References

[1] Huang M H, Mao S, Feick H, Yan H, Wu Y, Kind H, Weber E, Russo R and Yang P 2001 Room-temperature ultraviolet nanowire nanolasers *Science* **292** 1897–9
[2] Kaciulis S, Pandolfi L, Comini E, Faglia G, Ferroni M, Sberveglieri G, Kandasamy S, Shafiei M and Wlodarski W 2008 Nanowires of metal oxides for gas sensing applications *Surf. Interface Anal.* **40** 575–8
[3] Cha S N, Jang J E, Choi Y, Amaratunga G A J, Ho G W, Welland M E, Hasko D G, Kang D-J J and Kim J M 2006 High performance ZnO nanowire field effect transistor using self-aligned nanogap gate electrodes *Appl. Phys. Lett.* **89** 263102
[4] Wang Z L 2004 Nanostructures of zinc oxide *Mater. Today* **7** 26–33
[5] Fan Z, Wang D, Chang P-C, Tseng W-Y and Lu J G 2004 ZnO nanowire field-effect transistor and oxygen sensing property *Appl. Phys. Lett.* **85** 5923
[6] Hong W *et al* 2008 Tunable electronic transport characteristics of surface-architecture-controlled ZnO nanowire field effect transistors *Nano Lett.* **80** 950–6
[7] Chu S, Wang G, Zhou W, Lin Y, Chernyak L, Zhao J, Kong J, Li L, Ren J and Liu J 2011 Electrically pumped waveguide lasing from ZnO nanowires *Nat. Nanotechnol.* **6** 506–10
[8] Lu M-P, Song J, Lu M-Y, Chen M-T, Gao Y, Chen L-J and Wang Z L 2009 Piezoelectric nanogenerator using p-type ZnO nanowire arrays *Nano Lett.* **9** 1223–7
[9] Qu L, Dai L, Stone M, Xia Z and Wang Z L 2008 Carbon nanotube arrays with strong shear binding-on and easy normal lifting-off *Science* **322** 238–42

[10] Timm R, Persson O, Engberg D L J, Fian A, Webb J L, Wallentin J, Jönsson A, Borgström M T, Samuelson L and Mikkelsen A 2013 Current–voltage characterization of individual as-grown nanowires using a scanning tunnelling microscope *Nano Lett.* **13** 5182–9

[11] Léonard F, Talin A, Swartzentruber B and Picraux S 2009 Diameter-dependent electronic transport properties of Au-catalyst/Ge-nanowire Schottky diodes *Phys. Rev. Lett.* **102** 106805

[12] Lord A M, Maffeis T G, Walton A S, Kepaptsoglou D M, Ramasse Q M, Ward M B, Köble J and Wilks S P 2013 Factors that determine and limit the resistivity of high-quality individual ZnO nanowires *Nanotechnology* **24** 435706

[13] Lin Y, Li Q, Armstrong A and Wang G T 2009 *In situ* scanning electron microscope electrical characterization of GaN nanowire nanodiodes using tungsten and tungsten/gallium nanoprobes *Solid State Commun.* **149** 1608–10

[14] Li A-P, Clark K W, Zhang X-G and Baddorf A P 2013 Electron transport at the nanometer-scale spatially revealed by four-probe scanning tunnelling microscopy *Adv. Funct. Mater.* **23** 2509–24

[15] Qin S, Hellstrom S, Bao Z, Boyanov B and Li A-P 2012 Contacting nanowires and nanotubes with atomic precision for electronic transport *Appl. Phys. Lett.* **100** 103103

[16] Lord A M, Ward M B, Evans J E, Davies P R, Smith N A, Maffeis T G and Wilks S P 2014 Enhanced long path electrical conduction in ZnO nanowire array devices grown via defect-driven nucleation *J. Phys. Chem.* C **118** 21177–87

[17] Fian A, Lexholm M, Timm R, Mandl B, Håkanson U, Hessman D, Lundgren E, Samuelson L and Mikkelsen A 2010 New flexible toolbox for nanomechanical measurements with extreme precision and at very high frequencies *Nano Lett.* **10** 3893–8

[18] Lin Y-R, Tseng Y-K, Yang S-S, Wu S-T, Hsu C-L and Chang S-J 2005 Buffer-facilitated epitaxial growth of ZnO nanowire *Cryst. Growth Des.* **5** 579–83

[19] Fang Y, Wang Y, Wang Z and Sha J 2010 Detailed study on photoluminescence property and growth mechanism of ZnO nanowire arrays grown by thermal evaporation *J. Phys. Chem.* C **114** 12469–76

[20] Umar A, Kim S H, Lee Y S, Nahm K S and Hahn Y B 2005 Catalyst-free large-quantity synthesis of ZnO nanorods by a vapor–solid growth mechanism: structural and optical properties *J. Cryst. Growth* **282** 131–6

[21] Ho S-T, Chen K-C, Chen H-A, Lin H-Y, Cheng C-Y and Lin H-N 2007 Catalyst-free surface-roughness-assisted growth of large-scale vertically aligned zinc oxide nanowires by thermal evaporation *Chem. Mater.* **19** 4083–6

[22] Park W Il, Jung S W, Yi G-C, Oh S H, Park C G and Kim M 2002 Metal-ZnO heterostructure nanorods with an abrupt interface *Japan. J. Appl. Phys.* **41** L1206–8

[23] Lu W, Chen L and Fung W Y 2013 Vertical nanowire heterojunction devices based on a clean Si/Ge interface *Nano Lett.* **13** 5521–7

[24] Ozgur U, Alivov Y I, Liu C, Teke A, Reshchikov M A, Dogan S, Avrutin V, Cho S-J and Morkoc H 2005 A comprehensive review of ZnO materials and devices *J. Appl. Phys.* **98** 41301

[25] Soudi A, Hsu C-H and Gu Y 2012 Diameter-dependent surface photovoltage and surface state density in single semiconductor nanowires *Nano Lett.* **12** 5111–6

[26] Brillson L J, Mosbacker H L, Hetzer M J, Strzhemechny Y, Jessen G H, Look D C, Cantwell G, Zhang J and Song J J 2007 Dominant effect of near-interface native point defects on ZnO Schottky barriers *Appl. Phys. Lett.* **90** 102116

[27] Umar A, Karunagaran B, Suh E-K and Hahn Y B 2006 Structural and optical properties of single-crystalline ZnO nanorods grown on silicon by thermal evaporation *Nanotechnology* **17** 4072–7

[28] Wang Z, Kong X and Zuo J 2003 Induced growth of asymmetric nanocantilever arrays on polar surfaces *Phys. Rev. Lett.* **91** 185502

[29] Diebold U, Koplitz L V and Dulub O 2004 Atomic-scale properties of low-index ZnO surfaces *Appl. Surf. Sci.* **237** 336–42

[30] Tumakha S, Ewing D J, Porter L M, Wahab Q, Ma X, Sudharshan T S and Brillson L J 2005 Defect-driven inhomogeneities in Ni/4H–SiC Schottky barriers *Appl. Phys. Lett.* **87** 242106

[31] Sarpatwari K, Dellas N S, Awadelkarim O O and Mohney S E 2010 Extracting the Schottky barrier height from axial contacts to semiconductor nanowires *Solid-State Electron.* **54** 689–95

[32] Allen M W, Swartz C H, Myers T H, Veal T D, McConville C F and Durbin S M 2010 Bulk transport measurements in ZnO: the effect of surface electron layers *Phys. Rev.* B **81** 075211

[33] Suyatin D B *et al* 2014 Strong Schottky barrier reduction at Au-catalyst/GaAs-nanowire interfaces by electric dipole formation and fermi-level unpinning *Nat. Commun.* **5** 3221

[34] Gu Q L, Cheung C K, Ling C C, Ng A M C, Djurišić A B, Lu L W, Chen X D, Fung S, Beling C D and Ong H C 2008 Au/n-ZnO rectifying contact fabricated with hydrogen peroxide pretreatment *J. Appl. Phys.* **103** 093706

[35] Chaabouni F, Abaab M and Rezig B 2004 Metrological characteristics of ZnO oxygen sensor at room temperature *Sensors Actuators* B **100** 200–4